applied sciences

MDPI

Article

Analytical Investigation of Ricochet Range of Ogive—Shaped Nose Projectile Obliquely Penetrating Thick Steel Target

Yingxiang Wu [1], Xigui Tao [1] and Yijiang Xue [2,*]

[1] Institute of Defense Engineering, AMS, PLA, Beijing 100850, China; 1224846321@139.com (Y.W.); tonytxg@126.com (X.T.)
[2] State Key Laboratory of Explosion Science and Technology, Beijing Institute of Technology, Beijing 100081, China
* Correspondence: bitxue@bit.edu.cn

Abstract: The ricochet phenomenon has been studied worldwide for a long time in consideration of its significance in ballistics. A ricochet projectile has proven to be worthless to its launcher, as warheads fail to penetrate the interior of targets and strike the facilities and personnel of enemies effectively. A large portion of related research has been dedicated to avoiding ricocheting, which mainly focuses on improving the penetration ability of a projectile in order to obtain a better penetration effect, while investigations on the proactive protection of key targets from damage caused by a ricochet projectile are minor. This study analytically explores the ricochet range of a projectile obliquely penetrating a thick steel target. Firstly, the moment of momentum equation of the ricochet projectile based on theoretical mechanics is utilised to analytically calculate its trajectory, where a mathematical model of a two-stage ricochet impacting is established through the geometrical analysis of the ricochet process for determining the ricochet range of a projectile and the size of the bulletproof structure. Then, impact experiments of a projectile obliquely penetrating thick steel targets at different striking velocities and inclination angles are carried out, and the influences of the striking velocity and angle of attack on the damage pattern, area and penetration depth are discussed to identify the ricochet phenomenon. Moreover, the deflection angle of the ricochet projectile is computed, which is compared with the experimental measurements in order to validate the accuracy of this proposed model. This proposed research may promote security protection during live-firing training and provide a theoretical foundation for the optimisation of purposeful protection.

Keywords: ricochet; thick steel targets; moment of momentum equation; oblique penetration; impact experiment

check for updates

Citation: Wu, Y.; Tao, X.; Xue, Y. Analytical Investigation of Ricochet Range of Ogive—Shaped Nose Projectile Obliquely Penetrating Thick Steel Target. *Appl. Sci.* **2022**, *12*, 4692. https://doi.org/10.3390/app12094692

Academic Editor: Guian Qian

Received: 28 March 2022
Accepted: 1 May 2022
Published: 6 May 2022

1. Introduction

Although a great majority of experimentally ballistic data is gathered under ideal impact conditions of normal incidence, the probable fact is that almost all ballistic impacts occur at some non-ideal level of obliquity [1–6]. Goldsmith [7] comprehensively summarized analytical, numerical and experimental investigations of targets subjected to the nonstandard collisions, penetration and perforation of projectiles. Depending on projectile materials, shapes and speeds, as well as a host of different target substances, there will be a critical angle of obliquity beyond which the projectile will ricochet from the target surface. Ricochet is a special phenomenon in the oblique penetration of projectiles, where the projectile deflects from its course while maintaining its integrity after its impacting on the target [8,9]. The ricochet projectile proves worthless to its launcher, as its warhead fails to penetrate the interior of target and strike the facilities and personnel of the enemy effectively. Additionally, it may bring about the secondary impacting on an undesirable place [10]. This is highly manifested in the case of low-altitude or high-speed delivery modes against large steel targets like armoured fighting vehicles [11,12].

The ricochet phenomenon has been studied worldwide for a long time considering its significance in ballistics. Tate [13] developed an early model for the ricochet of rods based on the impacting of flat-nosed projectiles, which allows the local erosive deformation of the rod in the immediate vicinity of the impacting, where the asymmetric forces acting on this deforming rod tip are evaluated to ascertain their capacity to induce a rotation sufficient to bring about ricochet during the limited time before the rod tip becomes fully engaged in the target. Segletes [14] proposed a ricochet model based on the mechanics of materials-based approach, which focused on the interaction stresses and fluxes in the rod and target that produce the forces and moments required to continuously sustain a plastic hinge at the rod–target interface. However, Tate's model failed to predict the ricochet of rigid rods because of the method used to calculate the interaction force, and its requirement to ricochet by way of rigid rod rotation, and Segletes's model is represented by a handful of algebraic equations that must be simultaneously solved subject to various constraints. Currently, the analytical models concerning oblique incidence and ricochet are pitifully few and tend to be either extremely simple or limited to the initial stages of the impacting process. Therefore, it is essential to develop a relatively simplified model to not only meet the practical applications in engineering but also take into account the different stages of the impacting process.

Moreover, the ricochet problem can be investigated experimentally, and substantial studies concentrate on the governing factor in the generation of the ricochet and the penetration ability of the projectile. Sundararajan and Shewmon [15] studied the effects of the impacting angle, impacting velocity and dynamic hardness on the crater length and crater volume by impacting a hard ball against a semi-infinite target. Dikshit [1,2] conducted ballistic experiments to investigate the damage behaviour of a thick steel armour plate at different obliquities impacted by an ogive-shaped steel projectile. Extensive work has been carried out involving penetration and ricochet studies on thin metallic and composite plates impacted by hard balls, long rod penetrators and small arms ammunitions [16–29]. On the other hand, there exist several potential studies concerning the threat from ricochet projectiles or fragments, such as using shields to deflect space debris and meteorites of exploded projectiles or protecting critical equipment from intentional and accidental impacts [7,30]. However, studies pertinent to the protection of key targets from damages caused by projectile ricocheting have received less attention. Setting up a bulletproof board wall with uniform strength around the target is a conventional protective method, while this aimless prevention measure neither eliminates the threat of secondary damage from a ricochet projectile completely nor benefits from achieving an economical defence. Accordingly, it is significant to develop an effective way to predict the ricochet range of a projectile obliquely penetrating the target by utilizing ballistic prediction technology so as to identify the most critical area for battlefield protection and build a well-focused and flexible defence against ricochet projectiles.

In this study, the ricochet range of a projectile obliquely penetrating a thick steel target is purposefully investigated. Firstly, the moment of momentum (MM) equation of a ricochet projectile based on theoretical mechanics is utilized to analytically calculate its trajectory, where a mathematical model of two-stage ricochet impacting is established through geometrical analysis of the ricochet process for determining the ricochet range of the projectile and the size of the bulletproof structure. Then, impacting experiments of projectile obliquely penetrating thick steel targets at different striking velocities and inclination angles are carried out, and the influences of the striking velocity and angle of attack on the damage pattern, area and penetration depth are discussed to identify the ricochet phenomenon. Moreover, the deflection angle of the ricochet projectile is computed and compared with the experimental measurements in order to validate the accuracy of this proposed model. This proposed research may promote security protection in live-firing training and provide a theoretical foundation for the optimization of purposeful protection.

2. Mathematical Modelling of Ricochet

2.1. Geometrical Modelling

The process of a projectile obliquely penetrating the target is geometrically modeled considering a two-stage impacting of the ricochet. Figure 1 diagrams the trajectory of the projectile ricocheting from the target after its impacting on the target. During the geometrical analysis, MN stands for the target facing the projectile CA in the first impacting, and PN stands for the bulletproof wall impacted by the ricocheting projectile C_1A_1. Without a loss of generality, MN and PN are mirror symmetrically placed. In addition, A' and A_1' are the impacting points of the projectiles CA and C_1A_1 on the target and bulletproof wall, respectively.

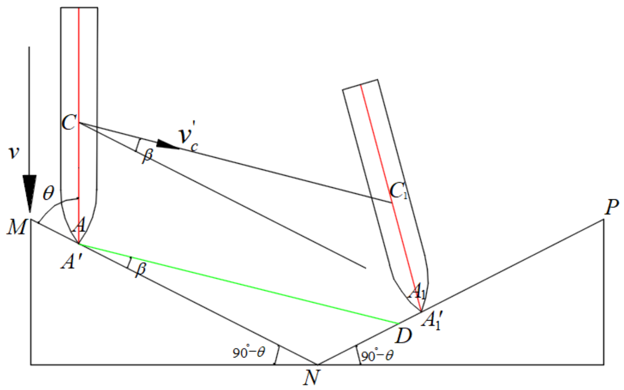

Figure 1. Geometric diagram of the projectile obliquely penetrating the target.

2.2. Momentum Analysis of Ricochet Process

The projectile and the target in the first impacting are analyzed as a whole, assuming that the projectile is rigid and without deformation while hitting the target. The axis of the projectile coincides with its initial flight velocity, and under the initial status and only the deflection force, the attacking angle of the projectile is zero. The coordinate system is set with the X axis parallel to MN and the Y axis perpendicular to MN.

On the basis of theoretical mechanics, the impacting analysis of the projectile is performed. Figure 2 displays the momentum in the process of first impacting, where the projectile with a mass of m and length of l obliquely penetrates the target with a velocity of v and incidence angle of θ. After the first impacting, the motion of the projectile is decomposed into a linear motion with a velocity consistent to that of its centre of mass and a rotation motion around its centre of mass. The MM equations of this system are expressed as:

$$mv_{cx}' - mv_{cx} = \sum I_x \tag{1}$$

$$mv_{cy}' - mv_{cy} = \sum I_y \tag{2}$$

$$J_C\omega_2 - J_C\omega_1 = \sum M_c\left(I^{(e)}\right) \tag{3}$$

where v_{cx} and v_{cy} are, respectively, the X and Y axial component of velocity of the centre of mass (VCM) of the projectile before the first impacting; v_{cx}', v_{cy}' are the X and Y axial components of the VCM of the projectile after the first impacting, respectively; I_x and I_y are impulses along the X and Y axis in the first impacting, respectively; J_C is the inertia moment of projectile about its centre of mass; ω_1 and ω_2 are, respectively, the angular velocity of the projectile before and after the first impacting; and $\sum M_c\left(I^{(e)}\right)$ is the vector sum of the angular impulse about the centre of mass (CM) of the projectile. Compared to its impulse, the gravity and aerodynamic drag force (moment) of the projectile can be neglected. Likewise, the projectile's drag force (moment) resulted from axially rotating, and its effects on the attacking angle and ballistic trajectory are negligible, because the projectile axis, deflecting force and velocity are all in the incident plane.

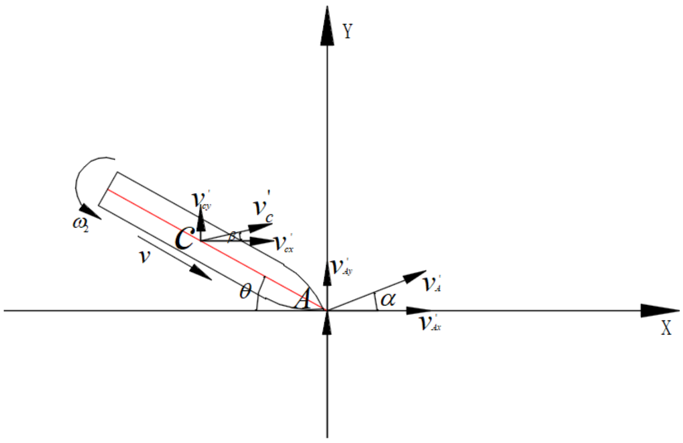

Figure 2. Momentum analysis in terms of the first impacting.

Before the impacting, the angular velocity ω_1 of the projectile is zero, and because the contact surface is smooth, the projectile impulse I_y along the Y axis in the first impacting is zero as well. The X axial component of the VCM after the first impacting is equal to that before the first impacting, and its corresponding expression is:

$$V'_{cx} = V_{cx} = V_c \cos\theta \tag{4}$$

When the material restitution coefficient e is introduced, the above formula can be written as:

$$ev_c \sin\theta = v'_{cy} + l' \cos\theta \cdot \omega_2 \tag{5}$$

Consequently, the analytical expressions of ω_2 and β can be derived as:

$$\omega_2 = \frac{ml'(e+1)v_c \sin 2\theta}{2(J_C + ml'^2 \cos^2\theta)} \tag{6}$$

$$\beta = \arctan\frac{v'_{cy}}{v'_{cx}} \tag{7}$$

2.3. Calculation of Ricochet Range

To conveniently define the motion trajectory of the projectile after the first impacting, new coordinate systems are established herein, which include a fixed and moving one. The X axis of the former is parallel to the direction of v'_c, and the Y axis is perpendicular to that. For the latter, the mass centre of the projectile after the t moment of the first impacting is C_1, where t is the time interval between two impacts. Figure 3 shows the diagram of the motion trajectory of the ricocheting projectile, and the equation of the relative movement trajectory (x', y') of its vertex is defined as:

$$\begin{cases} x' = l' \cdot \cos(\theta + \beta - \omega_2 t) \\ y' = -l' \cdot \sin(\theta + \beta - \omega_2 t) \end{cases} \tag{8}$$

where l' is the distance from the mass center to the vertex. By a coordinate transformation, the equation of absolute movement trajectory (x, y) of the vertex can be expressed as:

$$\begin{cases} x = v_c t + l' \cdot \cos(\theta + \beta - \omega_2 t) \\ y = l' \cdot [\sin(\theta + \beta) - \sin(\theta + \beta - \omega_2 t)] \end{cases} \tag{9}$$

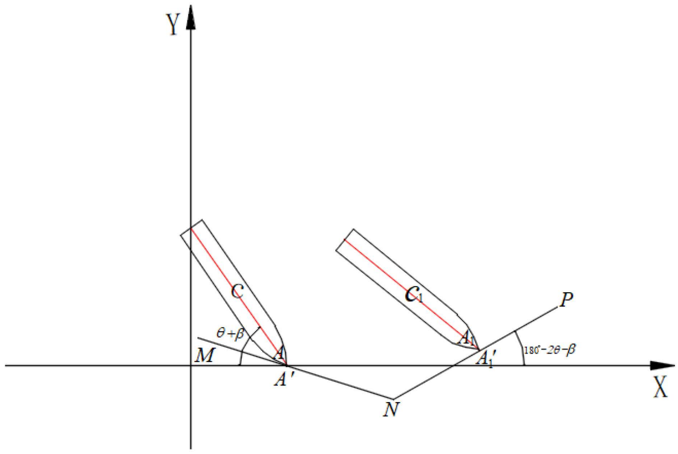

Figure 3. Diagram of the projectile trajectory in the ricochet process.

Similarly, the absolute movement trajectory (x_{PN}, y_{PN}) of the vertex in the ricochet process can be obtained. Moreover, the corresponding impacting point A_1' can be analytically determined when the two trajectories intersect each other.

2.4. Practical Application

Normally, the size of the target and the impacting point are predefined, but the location of the bulletproof structure is unknown, although it plays a key role in the protection of key targets from damages caused by projectile ricocheting. The aforementioned analytical method may contribute to finalizing the exact location of the bulletproof wall when the ricochet range is certain. A linear bulletproof wall PG is simply considered in Figure 4, where B is the impacting point of the projectile ricocheting. The equation of PG can be expressed as:

$$y = \tan\varpi\left[x - l' \cdot \cos(\theta+\beta) - s_1\right] \quad (10)$$

where ϖ is the angle between the PG and X axis, and s_1 is the distance from the incidence point A to K, which is the intersection of the PG and X axis. When Equations (9) and (10) are jointly computed, the relationship of t, ϖ and s_1 is derived as:

$$\frac{\sin(\theta+\beta) - \sin(\theta+\beta-\omega_2 t)}{\tan\varpi} = \cos(\theta+\beta-\omega_2 t) - \cos(\theta+\beta) - \frac{s_1 - v_c t}{l'} \quad (11)$$

$$t = f(\varpi, s_1) > 0 \quad (12)$$

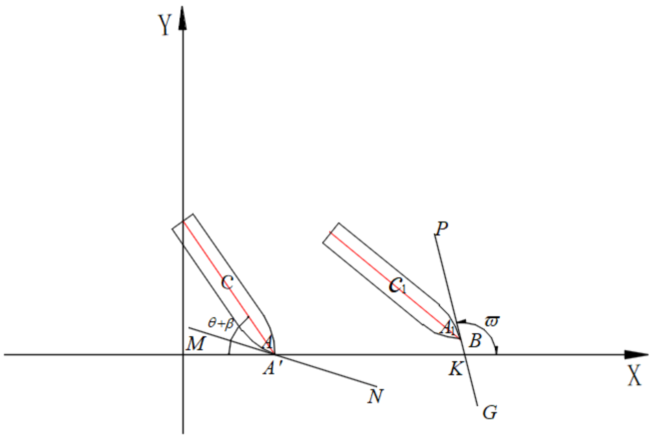

Figure 4. The diagram of a linear bulletproof structure.

The location of impacting point B can be obtained through trial calculations of (ϖ, s_1). The value of the inclination angle ϖ is limited by the site. When the bulletproof wall is set perpendicular to the target plate, ϖ reaches its maximum: $\varpi = 90 - \beta$. During the trial calculations, (ϖ, s_1) needs to be adjusted until Equation (11) can be solved. When Equation (11) has only one solution, the intersection is the impacting point $B(x_B, y_B)$. When Equation (11) has several solutions, the intersection matching the earliest moment is the impacting point $B(x_B, y_B)$.

Given that the incident angle may deviate from the designed value, B can be taken as the middle point of PG for security. When the intersection K is set as the middle point of BG, the size of the bulletproof wall can be calculated conveniently, and its size can be adjusted by multiplying a safety coefficient, taking into account the varying diameters of the projectile and materials of the target plate. Concerning the value of the safety coefficient, it will be disclosed in the subsequent research.

3. Experimental Setup

Impact experiments were carried out using a 40-caliber one-stage light-gas gun (Figure 5) of State Key Laboratory of Explosion Science and Technology of China located in the East Garden Test Base of Beijing Institute of Technology. The gun system includes a high-pressure chamber, a release valve, a projectile chamber and a barrel powered by a detonation reaction of hydrogen and oxygen, which promotes the energy utilization and loading efficiency of the gun. The maximum firing velocity of the light-gas gun varies with the mass of the projectile, and it drops as the mass of the projectile gets larger. In this experiment, the highest velocity is beyond 800 m/s, and the firing velocity can be altered by changing the pressure of the reaction gases.

Figure 5. A 40-caliber one-stage hydrogen-driven gas gun.

The targets made of 90-mm-thick-squared 45 steel plates with a cross-section of 500×500 mm^2 were impacted by alloy steel projectiles with ogival noses. The target plate was positioned approximately 10 m from the gun, and the inclination angle varied in the range of 0~45° (relative to the projectile line of flight). The projectile core was 30 mm in diameter, 120 mm long and weighed 466 g, with a hardness of HRC 49 (Figure 6). As the diameter of the projectile body was smaller than that of the gun barrel, the rod-shaped sabot made of high molecular weight polyethylene material was utilized to support the projectile body for accelerating its movement inside the barrel.

Figure 6. A 30-mm alloy steel projectile with an ogival nose.

The movement and deflection of the projectile was recorded with a time increment of 5 μs using a high-speed camera placed in front of the target. The frame number and resolution were, respectively, 10,000 and 1024 × 488, and the exposure time was 29.4 μs. The flight trajectory, attitude and speed of the projectile were obtained through analyzing the time-varying positions of the projectile. The impacting velocity was designed ranging from 300 m/s to 800 m/s. A wood board in place of a bulletproof wall was set at a certain distance away from the target plate to record the position of the impacting point of the ricochet. The distance between the impacting point on the target plate and that on the wood board was measured for further determining the deflection angle.

4. Experimental Results

4.1. Appearance of Impacted Plates and Damage Patterns

After the ballistic tests, each impacting site was subjected to detailed examination. The holes on the target plate and wood board were photographed, and the representative craters at different striking velocities and obliquities are presented in Figure 7. No damage was found on the back face of all the target plates (Figure 8), which could be assumed half-infinite. The fronts of the impacted plates were examined, and the damage patterns and the deformation mode of the plate during oblique penetration were defined. It can be noted that, due to the heavy heating effect and deformation, the flow of the material is the maximum and creates the petaling and crater damage patterns. Metal chipped away from the front surface by the projectile impacting under a lower attack angle is negligible.

(**a**) (**b**)

Figure 7. *Cont.*

(**c**) (**d**)

Figure 7. Typical appearance of craters of a 30-mm ogive-shaped steel projectile obliquely penetrating a 90-mm steel target plate at different striking velocities and obliquities: (**a**) 789 m/s, 15° obliquity; (**b**) 570 m/s, 25° obliquity; (**c**) 315 m/s, 30° obliquity and (**d**) 407 m/s, 45° obliquity.

Figure 8. Rear face of the target plate.

4.2. Damage Area

All the damage areas at the front face of the impacted plates were measured carefully after the ballistic impacting. First, with the help of trace paper, the impression of the damage areas was drawn on the paper. Then, putting it onto graph paper, the areas were measured. The damaged areas were plotted against the striking velocity at varying obliquities of impacting, and the results at a 30° angle of attack are shown in Figure 9. It could be observed that the damage area had a nearly linear increase with the increasing striking velocity. However, there were abrupt changes in the damaged area of the front face when a ricochet occurred. The maximum damage area was observed at the striking velocity of 398 m/s, while the minimum damage area was observed at the striking velocity of 411 m/s, and both of them were observed at a 30° angle of impacting. When the striking velocity was 398 m/s, the penetration depth was less than that of the projectile with a velocity of 411 m/s. Its possible cause was that the former flight projectile was mainly dominated by a lateral force, it grazed the target greatly, and the contact area was larger, but the latter one was controlled by a normal force, as the damage was mostly generated under the rebound action of the rigid body. In addition, dependent on the flight attitude of the projectile after firing, the damage power and area may have also made a difference.

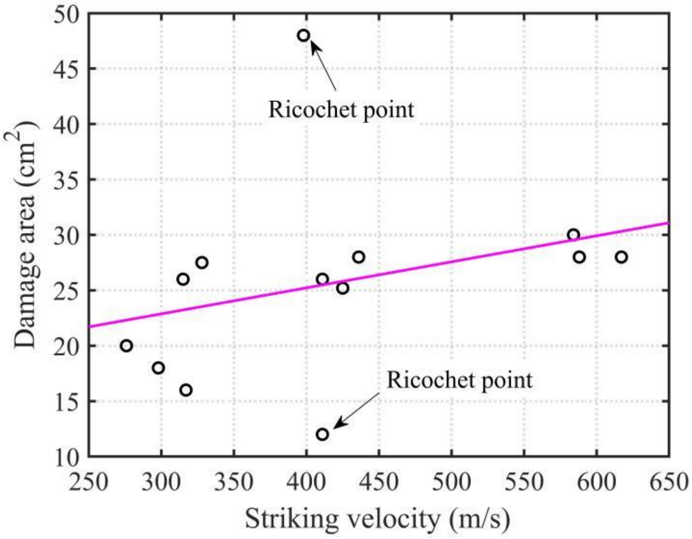

Figure 9. Variation of the damage area with the striking velocity at a 30° angle of attack.

4.3. Penetration Depth

The depths up to which the projectile penetrated into the target plates at different obliquities and velocities were experimentally measured. The results of the penetration depths varying with the striking velocity at 15° and 30° angles of attack were, respectively, compared with those from Dikshit (1998 and 1999), as displayed in Figure 10a,b, where T represents the thickness of the impacting plate, and D represents the diameter of the projectile.

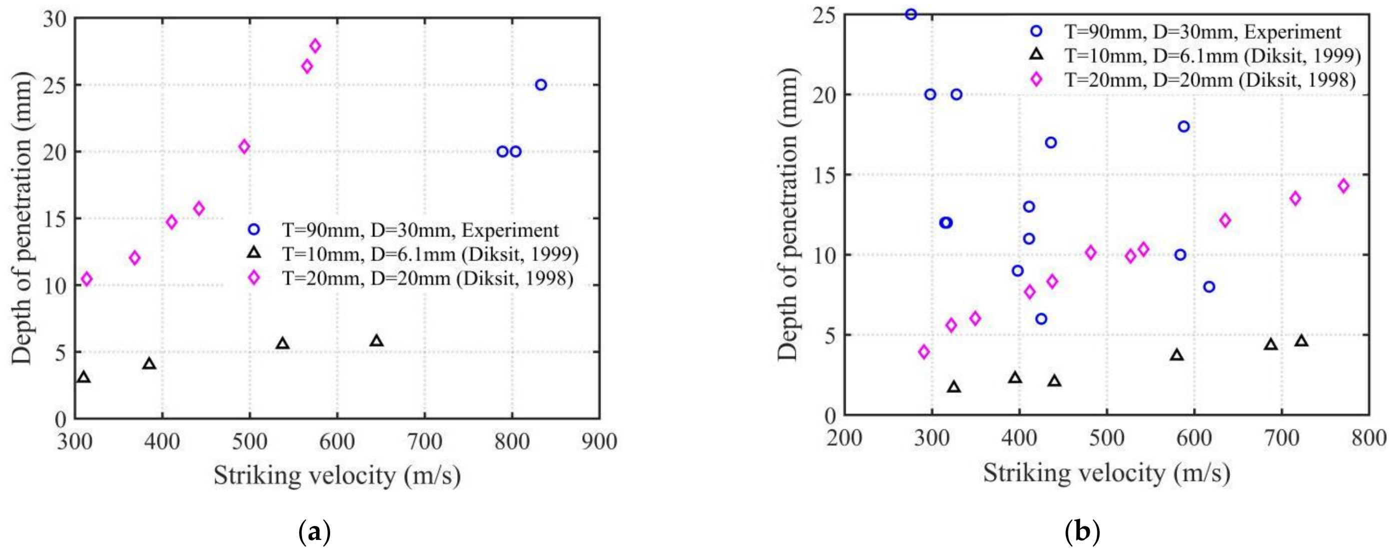

Figure 10. Variation of the penetration depth with the striking velocity at different obliquities: (**a**) 15° obliquity and (**b**) 30° obliquity.

It is observed that the penetration depth increases monotonically with the striking velocity of the projectile at 15° of impacting, but this seems unclear in term of the results at a 30° angle of attack, though Dikshit's studies indicated that "with increasing obliquity there is a decrease in the slope of the penetration curves". The plate behaviour indicates a decreasing penetration severity with the increasing angle of attack and reducing velocity, which is well within the ballistics expectations. However, the ricochet points are abnormal and at a lower striking velocity, so the depth of penetration may be larger. Moreover, the ballistics behaviour of the 90-mm plate on being impacted by a 30-mm-diameter steel projectile at different velocities is quite different from that of a 20-mm plate on being impacted by a 20-mm-diameter steel projectile, though the obliquity is identical. The likely reason for this difference is that both sides of target plates were perforated in Dikshit's experiments.

4.4. Validation of Ricochet Model

The data presented in Figures 9 and 10 clearly show that the penetration behaviour of the ricocheting projectiles can be quite different with the increasing velocity and obliquity. This kind of change in the ballistic behaviour of the impacting plate is basically related to the ricochet angle of the projectile. To validate the ricochet model, the ricochet points indicated in Figure 9 are used to calculate the deflection angle of the projectile, where the striking velocities are, respectively, 398 m/s and 411 m/s. The corresponding experimental results are presented in Figure 11. The average distance between the impacting point and the impacting point of the ricochet is equal to 51.25 cm. The measured deflection angles of the projectile are, respectively, 34.22° and 33.94°, and the deflection angle is calculated, where the material restitution coefficient e is 0.2 and the incidence angle θ is 60°. The graphical result of the analytical computation is displayed in Figure 12, where ω_2 =103.6 rad/s, $\beta = -28.56°$ and $\varpi = 61.44°$, and the equation of PG is defined as:

$$y = 1.84x - 1.16 \tag{13}$$

(**a**) (**b**)

Figure 11. Experimental results of the ricocheting projectile: (**a**) 398 m/s, 30° obliquity; (**b**) 411 m/s, 30° obliquity.

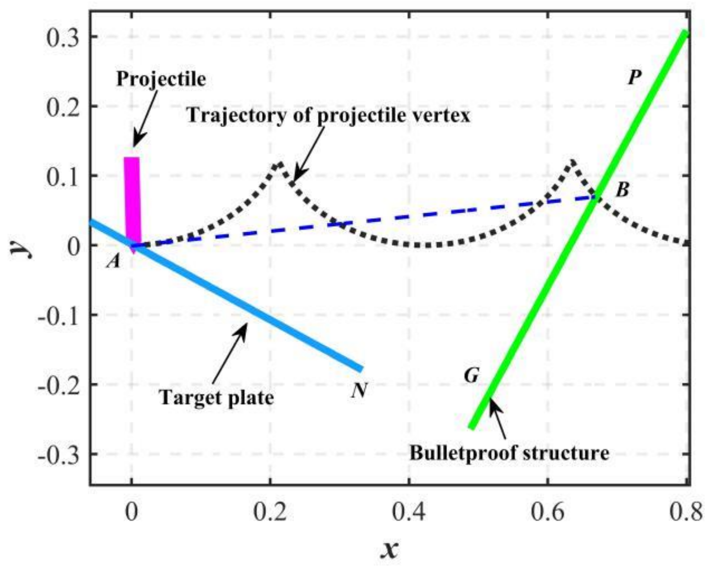

Figure 12. Graphical analysis of the ricocheting projectile and its deflection angle.

The coordinate of impacting point B is (0.67, 0.07); thus, the deflection angle (∠NAB) is 34.66°, which is the sum of β and the angle between line AB and the X axis, with an arc tangent of 0.07/0.67. Compared with the experimental results, the prediction error of the deflection angle is no larger than 2.1%.

To further verify the ricochet model, the experimental data from the ricochet tests conducted by Recht and Ipson et al. was utilized to compute the deflection angle, as cited in Figure 220 of Goldsmith's review paper [7], where the 12.7-mm-diameter, 26.5 g cylindroconical monobloc, spin-stabilized hardened steel projectiles with half-cone angles of 30° projectiles, were striking a 6.35-mm-thick armour plate of 230 BHN at 30° obliquity (namely θ = 60°) and an impact velocity of 343 m/s. As the ricochet obliquity $\beta_f = 54.44°$, the deflection angle was the complementary angle of β_f and equal to 35.56°. Correspondingly, the analytical calculating result was 37.85°, with $\omega_2 = 371.76$ rad/s, $\beta = -41.9°$. The prediction error of the deflection angle was 6.44%. The above comparative results demonstrate that the proposed model is accurate and can be an efficient tool to predict the trajectory and range of ricochet and optimize the design of bulletproof structures in engineering.

It should be noted that the ricochet model is not universal enough to explain all the problems related to the ricochet complex phenomenon. Additional data should be obtained to extend this model. At the present stage, a few assumptions involving rigid body movements are made, and the warhead shape and material properties are not fully considered, but this will be investigated thoroughly in the subsequent study. The model is established based on a momentum analysis, and it is assumed that the deformation of the projectile and target are both elastic plastic. This can be utilized to predict the movement trajectory of a ricochet projectile reasonably, which lays the foundation for optimizing the bulletproof structures. Compared with other existing complex analytical models, the advantage of this model is convenient for application and time-saving for computations.

5. Concluding Remarks

This study analytically determined the ricochet range of a 30-mm alloy steel projectile obliquely penetrating the thick steel target. The MM equation of a ricochet projectile based on theoretical mechanics was derived to calculate the motion trajectory of the vertex of a ricocheting projectile, where a two-stage ricochet impacting was modelled through a geometrical analysis of the ricochet process. The impacting point on the protective structure of the ricocheting was predicted through trial calculations, and the size of the bulletproof structure could be adjusted by a safety coefficient in view of the varying diameters of the projectile and materials of the target plate.

The ballistic experiments of ogive-shaped projectile obliquely penetrating thick steel targets at different striking velocities and inclination angles were conducted. The influences of the striking velocity and angle of attack on the damage pattern, area and penetration depth were investigated. No damage was found on the back faces of all the target plates, which could be assumed to be half-infinite. Due to a heavy heating effect and deformation, the flow of material was the maximum and created petaling and crater damage patterns on the front face, but the metal chipped away from the front surface by the projectile impacting under a lower attack angle was negligible. The damage area was nearly linearly increased with the increasing striking velocity, but there were abrupt changes in the damaged area of the front face when a ricochet occurred. The penetration depth increased monotonically, with a striking velocity of the projectile at a 15° impacting, but this seemed unclear at a 30° angle of attack. The penetration depth at a striking velocity of 398 m/s was less than that of the projectile with a velocity of 411 m/s. The possible cause was that the former flight projectile was mainly dominated by a lateral force, but the latter one was controlled by a normal force, where the damage was mostly generated under the rebound action of the rigid body. In addition, the flight attitude of the projectile after firing may have also made a difference. Moreover, the penetration depth increased monotonically with the striking velocity of the projectile at a 15° impacting, but this seemed unclear in terms of the results at the 30°angle of attack. The plate behaviour indicated a decreasing penetration severity with the increasing angle of attack and a reducing velocity. However, the ricochet points were abnormal and at a lower striking velocity, so the depth of penetration might get larger.

For validating the ricochet model, the ricochet points at the 30° angle of attack in the experiment were used to calculate the deflection angle of the projectile. Compared with the experimental results, the prediction error of the deflection angle was no larger than 2.1%, which demonstrated that the proposed model was accurate and could be an efficient tool to predict the trajectory and range of a ricochet and optimize the design of a bulletproof structure in engineering.

Author Contributions: Conceptualization, Y.X.; methodology, Y.W.; software, Y.W.; validation, Y.X., Y.W. and X.T.; investigation, Y.X., Y.W.; resources, Y.W. and X.T.; data curation, Y.X. and Y.W.; writing—original draft preparation, Y.W.; writing—review and editing, Y.X.; supervision, X.T. All authors have read and agreed to the published version of the manuscript.

Funding: This research received no external funding.

Conflicts of Interest: The authors declare no conflict of interest.

References

1. Dikshit, S.N. Ballistic behaviour of thick steel armour plate under oblique impacting: Experimental investigation. *Def. Sci. J.* **1998**, *48*, 271–276. [CrossRef]
2. Dikshit, S.N. Ballistic behaviour of thick steel armour plate under oblique impacting: Experimental investigation II. *Def. Sci. J.* **1999**, *49*, 257–262. [CrossRef]
3. Gupta, N.K.; Madhu, V. An experimental study of normal and oblique impact of hard-core projectile on single and layered plates. *Int. J. Impact Eng.* **1997**, *19*, 395–414. [CrossRef]
4. Hutchings, I.; Macmillan, N.; Rickerby, D. Further studies of the oblique impact of a hard sphere against a ductile solid. *Int. J. Mech. Sci.* **1981**, *23*, 639–646. [CrossRef]
5. Segletes, S.B. A model for rod ricochet. *Int. J. Impact Eng.* **2006**, *32*, 1403–1439. [CrossRef]
6. Segletes, S.B. Further development of a model for rod ricochet. *Int. J. Impact Eng.* **2007**, *34*, 899–925. [CrossRef]
7. Goldsmith, W. Non-ideal projectile impact on targets. *Int. J. Impact Eng.* **1999**, *22*, 95–395. [CrossRef]
8. Chen, X.; Lu, F.; Zhang, D. Penetration trajectory of concrete targets by ogived steel projectiles—Experiments and simulations. *Int. J. Impact Eng.* **2018**, *120*, 202–213. [CrossRef]
9. Jo, J.-H.; Lee, Y.-S. A Study of Ricochet Phenomenon for Inclined Impact of Projectile. *Int. J. Mod. Phys. Conf. Ser.* **2012**, *6*, 443–448. [CrossRef]
10. Venkatesan, N.S.; Kohli, S.L.; Battacharyya, A.R. A note on the determination of ricochet trace of small arms ammunition. *Def. Sci. J.* **1976**, *26*, 67–68.
11. Iqbal, M.; Khan, S.; Ansari, R.; Gupta, N. Experimental and numerical studies of double-nosed projectile impact on aluminum plates. *Int. J. Impact Eng.* **2013**, *54*, 232–245. [CrossRef]

12. Iqbal, M.; Senthil, K.; Bhargava, P.; Gupta, N. The characterization and ballistic evaluation of mild steel. *Int. J. Impact Eng.* **2015**, *78*, 98–113. [CrossRef]
13. Tate, A. A simple estimate of the minimum target obliquity required for the ricochet of a high speed long rod projectile. *J. Phys. D Appl. Phys.* **1979**, *12*, 1825–1829. [CrossRef]
14. Bassindowa, H.; Farouk, B.; Segletes, S.B. Impact and Ricochet of a High Speed Projectile from a Plate. *Def. Sci. J.* **2021**, *71*, 737–747. [CrossRef]
15. Sundararajan, G.; Shewmon, P. The oblique impact of a hard ball against ductile, semi-infinite target materials—Experiment and analysis. *Int. J. Impact Eng.* **1987**, *6*, 3–22. [CrossRef]
16. Dorogoy, A.; Rittel, D.; Brill, A. Experimentation and modeling of inclined ballistic impact in thick polycarbonate plates. *Int. J. Impact Eng.* **2011**, *38*, 804–814. [CrossRef]
17. Dorogoy, A.; Rittel, D.; Brill, A. A study of inclined impact in polymethylmethacrylate plates. *Int. J. Impact Eng.* **2010**, *37*, 285–294. [CrossRef]
18. Dou, Y.; Liu, Y.; Huddleston, B.; Hammi, Y.; Horstemeyer, M.F. A molecular dynamics study of effects of crystal orientation, size scale, and strain rate on penetration mechanisms of monocrystalline copper subjected to impacting from a nickel penetrator at very high strain rates. *Acta Mech.* **2020**, *231*, 2173–2201. [CrossRef]
19. Farouk, B.; Segletes, S.B. Ricochet of high speed aluminium projectiles from a steel plate. In Proceedings of the ASME 2016 International Mechanical Engineering Congress and Exposition (IMECE 2016), Phoenix, AZ, USA, 11–17 November 2016.
20. Goel, R.A.; Chandra, S.; Singh, H.; Abrol, A.K. Effect of L/D Ratio on Bomb Ricochet. *Def. Sci. J.* **1986**, *36*, 389–394. [CrossRef]
21. Johnson, W.; Sengupta, A.; Ghosh, S. High velocity oblique impact and ricochet mainly of long rod projectiles: An overview. *Int. J. Mech. Sci.* **1982**, *24*, 425–436. [CrossRef]
22. Daneshi, G.; Johnson, W. Forces developed during the ricochet of projectiles of spherical and other shapes. *Int. J. Mech. Sci.* **1977**, *19*, 661–671. [CrossRef]
23. Johnson, W.; Sengupta, A.; Ghosh, S. Plasticine modelled high velocity oblique impact and ricochet of long rods. *Int. J. Mech. Sci.* **1982**, *24*, 437–455. [CrossRef]
24. Lee, W.; Lee, H.-J.; Shin, H. Ricochet of a tungsten heavy alloy long-rod projectile from deformable steel plates. *J. Phys. D Appl. Phys.* **2002**, *35*, 2676–2686. [CrossRef]
25. Liu, Y.; Dou, Y.; Hammi, Y. Computational Investigation of High Velocity Penetration of Copper Subjected to Impact From Nickel Projectiles. In Proceedings of the ASME 2015-50241 International Mechanical Engineering Congress and Exposition, Houston, TX, USA, 13–19 November 2015.
26. Liu, Y.; Dou, Y.; Justin, W.; Horstemeyer, S.J.; Thirumalai, R.; Williams, W. Experimental Study of High Velocity Penetration of an Aluminum Target Plate by a Spherical Projectile. In Proceedings of the ASME 2015-50243 International Mechanical Engineering Congress and Exposition, Houston, TX, USA, 15–18 November 2015.
27. Muster, M.; Hameed, A.; Wood, D. Ricochet quantification using a multiple sensor approach. *Def. Technol.* **2021**, *17*, 305–314. [CrossRef]
28. Rosenberg, Z.; Surujon, Z.; Yeshurun, Y.; Ashuach, Y.; Dekel, E. Ricochet of 0.3″ AP projectile from inclined polymeric plates. *Int. J. Impact Eng.* **2005**, *31*, 221–233. [CrossRef]
29. Schultz, P.H.; Sugita, S.; Eberhardy, C.A.; Ernst, C.M. The role of ricochet impacts on impacting vaporization. *Int. J. Impact Eng.* **2006**, *33*, 771–780. [CrossRef]
30. Zukas, J.; Gaskill, B. Ricochet of deforming projectiles from deforming plates. *Int. J. Impact Eng.* **1996**, *18*, 601–610. [CrossRef]